TISSUE ENGINEERING: Part A
Volume 16, Number 10, 2010
© Mary Ann Liebert, Inc.
DOI: 10.1089/ten.tea.2010.0017

Alignment of Astrocytes Increases Neuronal Growth in Three-Dimensional Collagen Gels and Is Maintained Following Plastic Compression to Form a Spinal Cord Repair Conduit

Emma East, Ph.D., Daniela Blum de Oliveira, M.Sc., Jon P. Golding, Ph.D., and James B. Phillips, Ph.D.

After injury to the spinal cord, reactive astrocytes form a glial scar consisting of highly ramified cell processes that constitute a major impediment to repair, partly due to their lack of orientation and guidance for regenerating axons. In some nonmammalian vertebrates, successful central nervous system regeneration is attributed to the alignment of reactive glia, which guide axons across the lesion site. Here, a three-dimensional mammalian cell-seeded collagen gel culture system was used to explore the effect of astrocyte alignment on neuronal growth. Astrocyte alignment was mapped within tethered rectangular gels and was significantly greater at the edge and middle of the gels compared to the control unaligned regions. When neurons were seeded on and within astrocyte gels, neurite length was greatest in the areas of astrocyte alignment. There was no difference in expression of astrocyte reactivity markers between aligned and control areas. Having established the potential utility of astrocyte alignment, the aligned gels were plastic compressed, transforming them into mechanically robust implantable devices. After compression, astrocytes remained viable and aligned and supported neurite outgrowth, yielding a novel method for assembling aligned cellular constructs suitable for tissue engineering and highlighting the importance of astrocyte alignment as a possible future therapeutic intervention for spinal cord repair.

Introduction

In the undamaged central nervous system (CNS), there is a highly organized continuous longitudinal and transverse arrangement of glial cells,[1] which is disrupted after injury. The glial scar that forms after spinal cord injury (SCI) is considered a physical and physiological impediment to neuronal regeneration. It is composed largely of reactive, hypertrophic astrocytes, which up-regulate intermediate filaments including glial fibrillary acidic proteins (GFAP) and vimentin and deposit chondroitin sulfate proteoglycans (CSPGs), allowing them to become ramified and inhibitory to axonal growth.[2–4] It is likely that the physical barrier of disorganized astrocytes in the glial scar, which also forms around tissue-engineered devices and grafts implanted to aid repair, may act to disrupt guidance of regenerating axons, adding to the overall inhibition of axonal growth. The result is that although axons readily enter and traverse bridging grafts, they rarely exit the graft to re-integrate robustly with the host parenchyma.[5]

By contrast, in nonmammalian vertebrates such as amphibians, regeneration of axons occurs directly through dense glial scar tissue.[6] This can be largely attributed to the arrangement of reactive glial cells, which form organized channels, creating pathways for regenerating axons to bridge a lesion.[7] In recent SCI research, using cell therapies in rodents, successful growth of axons was observed in association with aligned glial cells.[8–10] The contribution of this alignment has tended to be downplayed due to interest in the molecular environment whose role in neuronal inhibition is better understood *in vivo*. However, the complexity of *in vivo* models makes it difficult to isolate this variable, thus failing to establish the contribution of alignment when interpreting results.[11] It is tempting to speculate that organized conduits of aligned astrocytes may improve regeneration after SCI.

Previous *in vitro* studies have investigated how alignment of astrocytes can affect regenerating neurites (reviewed by East *et al.*[12]). Astrocytes have been manipulated to create longitudinally aligned monolayers either by application of mechanical

Preliminary forms of this work were presented at (1) Tissue and Cell Engineering Society, Glasgow, June 2009 and (2) Glial cells in Health and Disease, Paris, September 2009.
Department of Life Sciences, The Open University, Walton Hall, Milton Keynes, United Kingdom.

strain or through the influence of surface architecture, for example, micropatterned grooves.[13–16] In these studies, alignment of astrocytes directed and enhanced the growth of neurites over their surface; however, investigations of this phenomenon have been limited to two-dimensional (2D) culture experiments. The relevance of 2D cultures is becoming increasingly questionable when tackling complex three-dimensional (3D) biological problems such as understanding the response to CNS injury. The mature glial scar, a meshwork of interwoven astrocytes processes, is a 3D structure.[17] Monolayer cultures fail to reproduce the 3D spatial arrangement of cells *in vivo*, polarize cell attachment and perfusion to opposite faces of the cell, and generally confer a considerably stiffer substrate environment than the endogenous extracellular matrix.[12,18–22] Recently, we developed a 3D collagen gel model for studying astroglial biology that has significant advantages over standard 2D models, allowing astrocytes to behave in a way much more reminiscent of their *in vivo* counterparts.[23] Since 3D culture systems can allow mechanical cues to be isolated from chemical cues,[24] we have adapted our 3D culture model in this study to explore the effect of astrocyte alignment on neurite growth.

Although a number of methodologies exist to align collagen, for example, magnetic and electrical fields and shear flow,[25–28] we used a tethered self-aligning model.[29] This system has the advantage that the cells themselves create simultaneous alignment of both cells and matrix. Cells seeded in collagen gels form stable integrin-mediated attachments with the fibrils of the compliant collagen lattice and generate forces that contract the gel.[29] Cellular contraction of a tethered rectangular gel creates a region in which tension is parallel with the long axis of the gel, leading to cell alignment along this axis. The gel also has unaligned triangular "delta" zones at either end, which are more isotropic due to stress shielding from the rigid tethering bars.[30] This means that both aligned and nonaligned regions can be compared within the same gel, providing a powerful model system in which cellular alignment can be isolated from other variables. The aim of this work was to map astrocyte alignment within tethered collagen gels, determine the effect of astrocyte alignment on neurite outgrowth, and then develop an implantable device that could provide an aligned glial environment to bridge the damaged spinal cord.

Materials and Methods

Astrocyte cell culture

All experiments were performed according to the UK Animals (Scientific Procedures) Act (1986) and approved by the Open University animal ethics advisory group. Sprague–Dawley rats (a β-actin-green fluorescent protein reporter line or wild type) were used from established in-house breeding colonies. Primary astrocyte cultures were prepared from postnatal 2-day-old rat cortices.[31] Briefly, the tissue was chopped and incubated with 250 μg/mL trypsin (Sigma) for 15 min at 37°C before addition of soya bean trypsin inhibitor (21 μg/mL; Sigma) and deoxyribonuclease 1 (6 μg/mL; Sigma). After centrifugation for 2 min at 250 *g*, the pellet was triturated in a concentrated solution of soya bean trypsin inhibitor and deoxyribonuclease 1 (133 and 40 μg/mL, respectively). The resulting cell suspension was underlain with 4% w/v bovine serum albumin, then centrifuged at 250 *g* for 5 min. The pellet was resuspended in Dulbecco's modified Eagle's medium (DMEM; Gibco) supplemented with penicillin or streptomycin (100 U/mL and 100 μg/mL, respectively; Sigma) and 10% v/v fetal calf serum and dispensed into 75 cm^2 flasks (Greiner) coated with poly-D-lysine (Sigma). Cultures were maintained in a humidified incubator at 37°C with 5% CO_2:95% air.

Dorsal root ganglia preparation and culture

Dorsal root ganglia (DRG) were dissected from adult rats (200–300 g). Nerve roots were stripped and DRGs were incubated in collagenase (0.125%; Sigma) for 2 h at 37°C. Tissue was dissociated by trituration and washed twice by centrifugation with 25 mL of media to remove any remaining collagenase. Cell pellets were resuspended in DMEM and seeded onto astrocyte and fibroblast coculture gels or mixed in with the astrocytes and fibroblasts during gel formation.

Neural fibroblast cultures

Neural fibroblasts were prepared from the sciatic nerves of adult rats (200–300 g) according to Phillips *et al.*[32] Sterile phosphate-buffered saline was used to wash the nerves before careful removal of the epineurial and perineurial sheath. The remaining endoneurium was chopped into 1 mm lengths and incubated in DMEM for 1 week in a humidified incubator at 37°C, with 5% CO_2, 95% air. After a 20 h incubation in collagenase (0.125%), tissue was dissociated; and the resulting cell suspension was plated into flasks coated with poly L-lysine (20 μg/mL; Sigma). After two passages, all cells were thy-1.1-immunoreactive fibroblasts.

3D tethered astrocyte cultures

Astrocytes and fibroblasts were expanded in culture for 8 days to reach confluence. Flasks containing astrocytes were shaken at 150 rpm for 4 h to detach microglia and less adherent cells from the cultures. Resulting cultures were 95% astrocytes and 5% microglia (as determined by immunoreactivity for GFAP and IB4 lectin, respectively). Cells were trypsinized, washed, and counted so that the correct densities could be calculated. For 3D cultures used in the modeling experiments, astrocytes were seeded at 2 million cells/mL, and neural fibroblasts were added at 5% (100 k/mL) to ensure consistent gel contraction. Rectangular tethered collagen gels were created according to methods previously described[29,33] within stainless steel moulds (Fig. 1A). Gels were composed of 10% cell suspension in DMEM, 10% 10× minimum essential medium (Sigma), and 80% type I rat tail collagen (2 mg/mL in 0.6% acetic acid; First Link). The minimum essential medium and collagen were mixed together and neutralized using sodium hydroxide, assessed by color change of phenol red pH indicator, then the mixture was added to the cell suspension and transferred to the moulds. One milliliter of gel was added per mould (Fig. 1B), ensuring that the gel mixture fully integrated with the mesh tethering bars, then cultures were left to set (~5 min), before topping up with 8 mL DMEM supplemented with penicillin or streptomycin and 10% fetal calf serum. Cultures were incubated at 37°C, with 5% CO_2 and 95% air for 3 days to contract (Fig. 1C) before fixing in 4% paraformaldehyde.

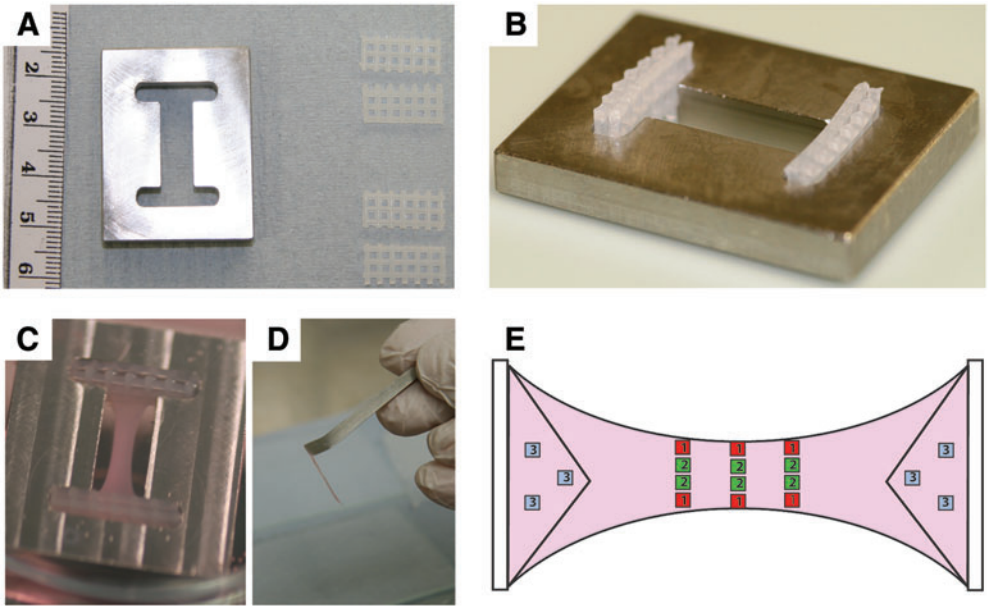

FIG. 1. Three-dimensional collagen gel preparation and data capture. (**A**) Stainless steel mould and tethering bars used for self-aligning tethered gels. (**B**) Metallic mould with the tethering bars positioned. The tethering bars are placed at each end of the metallic moulds so that when the collagen gel is added to the mould, the gel will integrate with the bars. (**C**) Contracted, aligned gel containing astrocytes in culture. (**D**) Aligned astrocyte-seeded device after plastic compression and rolling. (**E**) Diagram of the contracted collagen gel demonstrating the different regions of the gel that were analyzed. Red fields labeled 1 represent the edges of the gel; green fields labeled 2 represent the middle of the gel; and blue fields labeled 3 represent the delta zones. Color images available online at www.liebertonline.com/ten.

Plastic compression of aligned astrocyte devices

To generate implantable constructs containing aligned astrocytes, plastic compression was carried out as described [34,35] on aligned astrocyte cultures that had been stimulated to contract using transforming growth factor β1 (10 ng/mL) rather than 5% fibroblasts. This was to avoid the need to include fibroblasts, therefore simplifying the number of different cellular components required to make a potential repair conduit. Transforming growth factor β1 (10 ng/mL) can trigger astrocytes to become chronically activated over 10–15 days in culture (East *et al.*, 2009)[23]; however, here 48 h treatment was sufficient to induce contraction of the gels and cellular alignment. Plastic compression was achieved by loading the gel with 120 g for 1 min with fluid removal into a porous paper pad.[34] Resulting compressed sheets containing aligned astrocytes were ~40 μm thick and were rolled around their long axis to form a rod-like construct (Fig. 1D). Dissociated DRGs were cultured on the devices for 3 days and were then fixed in 4% paraformaldehyde.

Cell viability. To investigate the effect of plastic compression on cell viability, live dead staining was performed on gels using Hoechst 33258 (1 μg/mL) and propidium iodide (20 μg/mL; Sigma), as previously described.[23] This compared cell death in three compressed gels (1 h after compression) to cell death in three uncompressed gels.

Immunofluorescence staining and microscopy

Antibody sources, dilutions, and immunofluorescence staining were carried out as previously described.[23] Gels were stained for GFAP and βIII tubulin (astrocytes and neurons, respectively), and Hoechst 33258 was used to label cell nuclei. Analysis of immunostained gels was performed according to Figure 1E, where region 1 is the gel edge, region 2 is the middle of the gel, and region is 3 the delta zone. Six fields were viewed per region per gel, using an automated analysis protocol, focusing on the top of the gels for neurite measurements when neurons were seeded on the top, and within the center of the gels for astrocyte alignment and for neurite measurements when neurons were seeded within the gels. Six independent gels were analyzed per condition. Images were captured using an Olympus BX61 microscope with Analysis® Pro imaging software, (Olympus Soft Imaging System) or a Leica DMIRBE confocal microscope (Leica Microsystems). For confocal microscopy, *Z* stacks were 25 μm, with 1 image per 1 μm in the *Z* direction.

Image analysis

Astrocyte alignment. Astrocyte alignment was measured with Openlab Software (Improvision). A color density slice was performed on thresholded images to separate astrocytes as individual objects. The aspect ratio of individual cells relative to the gel axis was used as an index of cellular alignment. A population of unaligned cells would have a wide range of aspect ratios, whereas elongated aligned cells would be longer in one direction. Individual cells were plotted on a scatter graph for length (x) against width (y), and a linear regression was performed for each gel region. The alignment index was calculated by subtracting 1 from the inverse of the gradient of the line of best fit.

Neurite outgrowth. The length of βIII-tubulin immunostained neurons was measured with Openlab Software (Improvision), and the number of neurites per neuronal cell body was counted. Only neurites that were entirely within the field of each image were included in the analysis. The number of neurites measured per gel ranged from 147 to 202, with six independent gels per condition.

Reverse transcriptase (RT)-polymerase chain reaction

Protocol and primer sequences were as previously described.[23] Briefly, RNA was isolated using Trizol according to manufacturer's instructions. Equivalent amounts of RNA were reverse transcribed into single-stranded cDNA (3 μg per sample). Polymerase chain reaction (PCR) was performed on 100 ng cDNA per sample for GFAP, neurocan, and glyceraldehyde 3-phosphate dehydrogenase. PCR products were run on 1% agarose gels against a 100 bp DNA ladder.

Statistical analysis

Data were analyzed with GraphPad Prism software (Version 4). A paired *t*-test was used with significance level 95% for comparison of astrocyte alignment and mean neurite lengths in different areas of the gels. An unpaired *t*-test was used with significance level 95% for comparison of gels with and without astrocytes. If variances of data sets were significantly different, then Welch's correction was applied. All values are indicated as mean ± standard error of the mean.

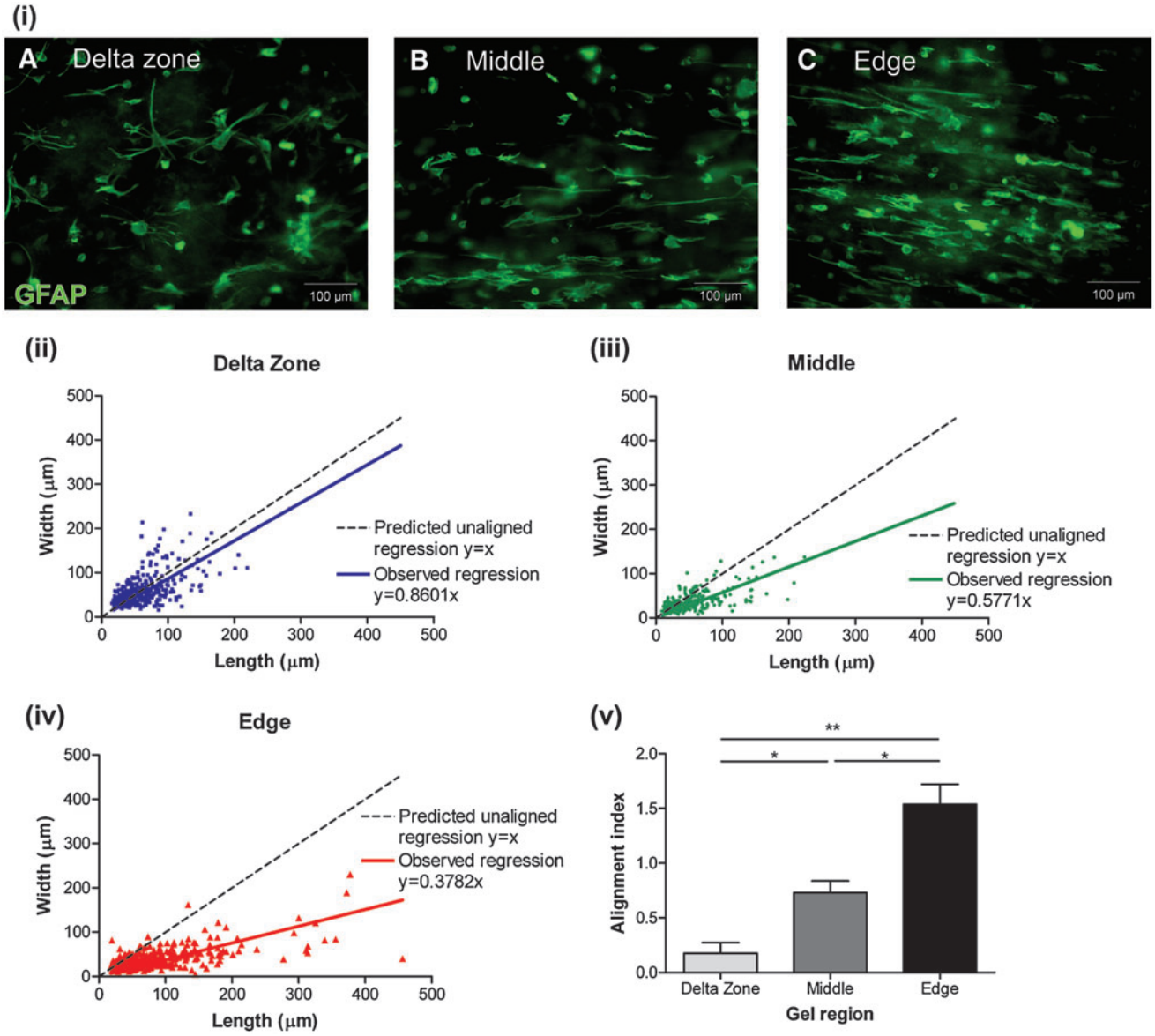

FIG. 2. Astrocytes become aligned in the middle and edges of tethered three-dimensional collagen gels. (**i**) Astrocytes stained for GFAP in the three different areas of the gels; delta zone (**A**), middle (**B**), and edges (**C**). The aspect ratio (cell length vs. width) of astrocytes was measured as an indicator of alignment in the delta zone (**ii**), middle (**iii**), and edge (**iv**) of the gels. If a population of cells is unaligned, then they are predicted to have equivalent length and width overall (predicted regression $y = x$). The cells in the delta zone did not differ significantly from the unaligned prediction. However, cells in the edges of the gels were significantly more aligned than those in the middle of the gels, which were significantly more aligned than cells in the delta zone. (**v**) Alignment index. $n = 6$ independent gels, $^{*}p < 0.05$, $^{**}p < 0.01$. GFAP, glial fibrillary acidic proteins. Color images available online at www.liebertonline.com/ten.

p-Values were taken as an indicator of statistical significance as follows: $*p < 0.05$, $**p < 0.01$, and $***p < 0.001$.

Results

Mapping astrocyte alignment

Using immunofluorescence to detect GFAP, it appeared that in the delta zones of the gels there was no astrocyte alignment [Fig. 2(i) A], whereas some alignment was observed in the middle and edges of the gels [Fig. 2(i) B, C]. Cell density in all gel regions did not significantly differ (data not shown). To quantify this observation, the degree of astrocyte alignment was determined by measuring cell aspect ratio. Overall, a population of unaligned cells would have equivalent width (y-axis) and length (x-axis) shown as a black dotted line in Figure 2(ii), (iii), and (iv). The linear regression plotted for astrocytes in the delta zone was not significantly different from the unaligned prediction [Fig. 2(ii)], indicating no astrocyte alignment in this region. This confirmed that the delta zones can be used as internal control regions to compare aligned and unaligned areas in the same gels.[29] By contrast, a significant increase in astrocyte alignment along the long-axis of the gel ($x > y$) was observed in the middle and edges of the gels when compared with the delta zones [Fig. 2(iii), (iv), respectively; $p < 0.001$]. At the edges of the gels, cell length was on average 2.5 times greater than cell width. For each region within each gel, a regression was performed and for each gel ($n = 6$) the alignment index was calculated. Astrocytes at the edges of the gels were significantly more aligned than those in the middle of the gels, which, in turn, were significantly more aligned than those in the delta zone [Fig. 2(v); $p < 0.05$].

Astrocyte alignment does not alter expression of reactivity markers

Increased production of CSPGs contributes to the inhibitory environment of the glial scar and is attributed to the failure of axon regeneration.[36] To determine whether there were differences in astrocyte reactivity between aligned and unaligned regions, RT-PCR and immunostaining were performed for CSPGs and GFAP. Levels of mRNA for GFAP and a neurite growth-inhibitory astrocyte-specific CSPG, neurocan, did not differ substantially between aligned and delta zone gel regions [Fig. 3(i)]. This corresponded to results using immunofluorescence where there were no apparent differences in the levels of GFAP and CSPGs detected in the gels between aligned and delta zone regions [Fig. 3(ii) A, B]. CSPG immunoreactivity was seen in association with aligned astrocytes and deposited in the surrounding matrix [Fig. 3(ii) A]. In some gel regions, this matrix-associated CSPG appeared aligned, but this was not consistently detected in any particular region and was not always associated with the presence of aligned astrocytes.

Neurite outgrowth on top of 3D tethered astrocyte cultures increased in areas of alignment

Dissociated DRG neurons were seeded onto the top surface of 3D tethered astrocyte cultures and maintained for 3 days. Gels were stained for βIII tubulin [Fig. 4(i) A–C] and GFAP [Fig. 4(i) D–F] for neurons and astrocytes, respectively, and Hoechst [Fig. 4(i) G–I] for cell nuclei. Nuclei that were neither GFAP nor βIII-tubulin positive could be either fibroblasts or DRG satellite glia. In unaligned delta zone regions, neurons extended neurites with random orientations [Fig. 4(i) G]. However, in the middle and edges of the gels, neurites extended in an orientated manner, along the same axis as the astrocyte alignment [Fig. 4(i) H, I]. In the delta zones, 80% of neurites extended between 0 and 200 μm. In contrast, at the edges of the gels, only 35% of neurites measured 0–200 μm, and instead the majority of neurites (65%) were ≥200 μm [Fig. 4(ii)]. In addition, the mean length of neurites at the gel edges was 192.6 ± 4.5 μm, significantly greater than 143.4 ± 2.5 μm in the delta zones [Fig. 4(iii); $p < 0.01$]. Although neurite length appeared increased in the middle of the gels compared with the delta zones, this did not reach statistical significance.

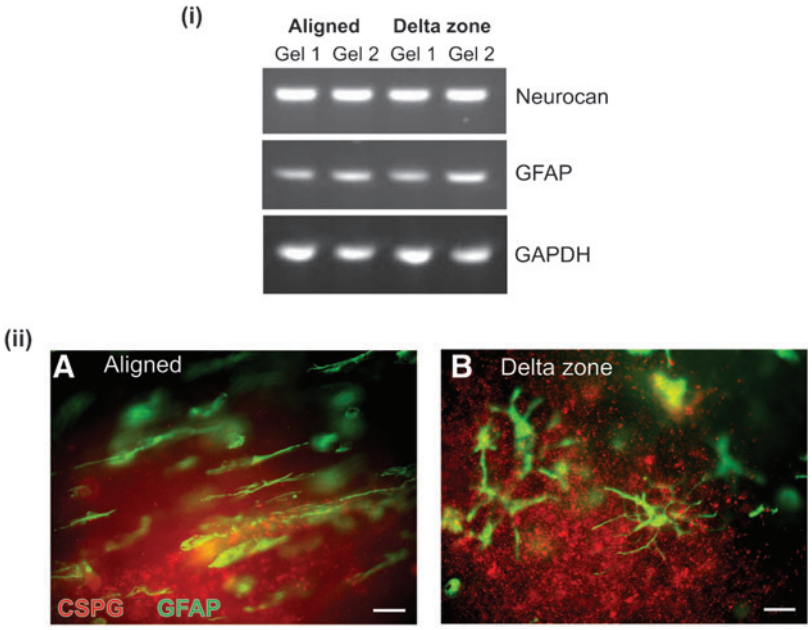

FIG. 3. Levels of GFAP and CSPGs are equivalent in regions of aligned and unaligned astrocytes. (**i**) Using RT-polymerase chain reaction, the expression of GFAP and the astrocyte-specific CSPG neurocan were compared, using GAPDH expression as a reference control. There were no substantial differences in the levels of the message for these proteins between the aligned and delta zone regions of the gel. (**ii**) There were no apparent differences in immunofluorescence for GFAP and CSPGs in the aligned (**A**) or delta zones (**B**) of tethered astrocyte gels. Scale bars in (**A**) and (**B**) = 25 μm. CSPG, chondroitin sulfate proteoglycan; GAPDH, glyceraldehyde 3-phosphate dehydrogenase. Color images available online at www.liebertonline.com/ten.

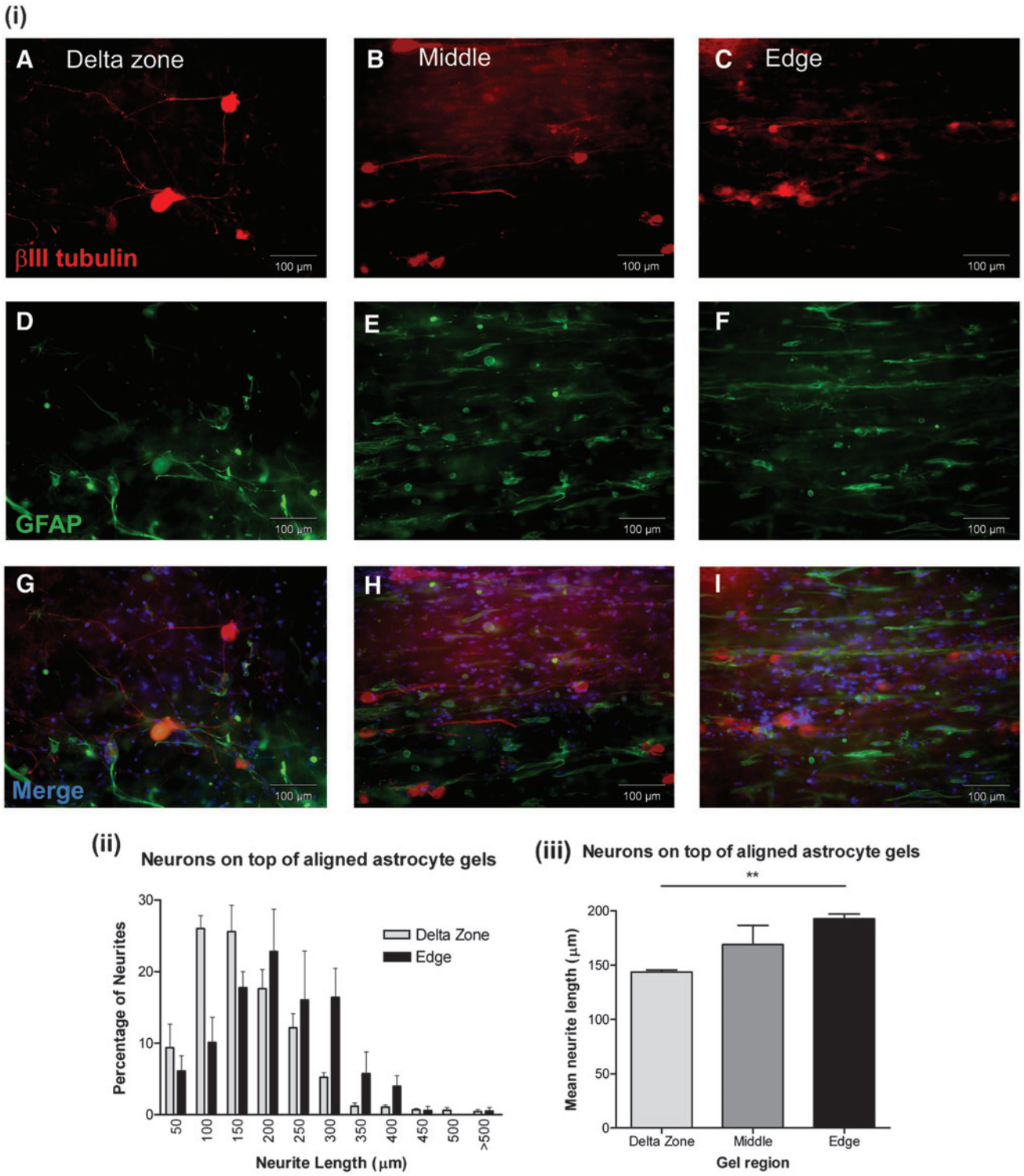

FIG. 4. Neurite extension on top of astrocyte cultures increased in areas of alignment. (**i**) Neurons and astrocytes stained for βIII tubulin (**A–C**), GFAP (**D–F**) and merged images, including Hoechst nuclear stain (**G–I**) in the delta zone, middle and edges of tethered collagen gels. (**ii**) Frequency distribution of neurite lengths in edge and delta zone locations reveals a shift to longer neurite lengths in the edge regions. (**iii**) The mean length of neurites was significantly greater at the edges of gels compared with the delta zones. $n = 6$ independent gels, $^{**}p < 0.01$. Color images available online at www.liebertonline.com/ten.

Alignment enhanced and directed neurite outgrowth within 3D tethered astrocyte cultures

Having established the ability of aligned astrocytes to promote neurite growth when DRG neurons were seeded on the surface of gels, studies were conducted to investigate neuronal growth within a 3D aligned astrocyte environment. Dissociated DRGs were mixed within astrocyte gels before setting. The gels were then left to align and grow in culture over 3 days, before fixing and staining for βIII tubulin. Similar to the previous experiment, in the delta zones neurons extended neurites randomly [Fig. 5(i) A]. However, in the middle and edges of the gels, neurites grew along the same axis as the astrocyte alignment [Fig. 5(i) B, C]. Again, neurons

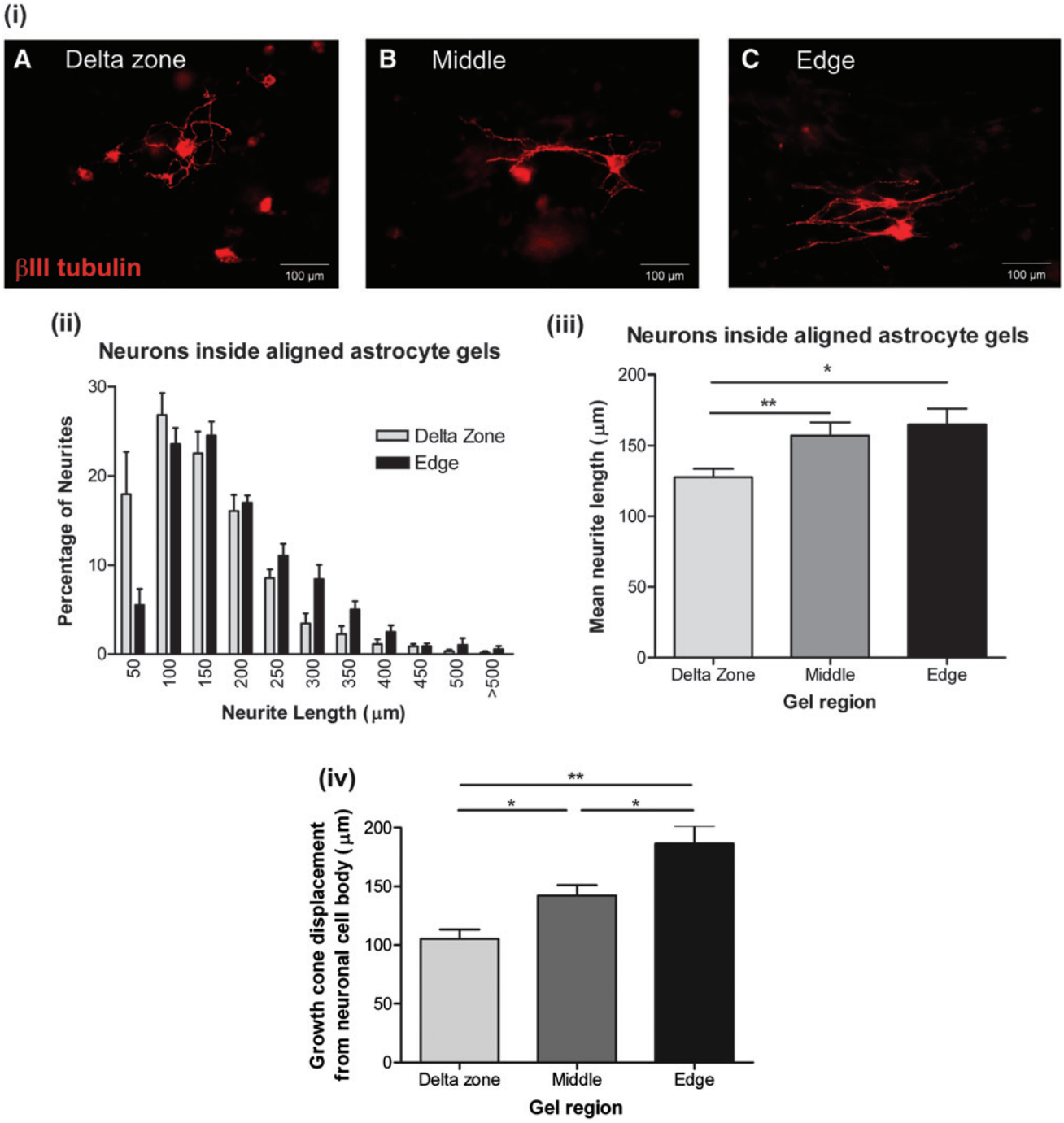

FIG. 5. Neurite extension within astrocyte cultures increased in areas of alignment. (**i**) Images show neurons stained for βIII tubulin within tethered gels (**A–C**). (**ii**) Frequency distribution showing the percentage of neurites of different lengths within tethered astrocyte gels. (**iii**) The average length of neurites within tethered astrocyte gels is significantly greater in the middle and at the edges of gels compared with the delta zones. (**iv**) Distance of the growth cone from the neuronal cell body is significantly greater at the middle and edges of the gels. $n = 6$ independent gels, $^{*}p < 0.05$, $^{**}p < 0.01$. Color images available online at www.liebertonline.com/ten.

extended shorter neurites in the delta zones, with 70% having lengths of between 0 and 150 μm [Fig. 5(ii)]. By contrast, in the edges of the gels, 70% of neurons had neurites that extended for ≥150 μm [Fig. 5(ii)]. The average length of neurites was 157.1 ± 9.3 μm in the middle of the gels and 164.8 ± 11.3 μm at the gel edges, both significantly greater than that in the delta zones [Fig. 5(iii); $p < 0.01$ and $p < 0.05$, respectively]. Growth cones in the middle and edges of the gels had extended significantly further away from the neuronal cell body (142.3 ± 8.9 and 186.7 ± 15.1 μm, respectively) than those in the delta zones, which, on average, were only 105.4 ± 8.0 μm from the cell body [Fig. 5(iv); $p < 0.05$ and $p < 0.01$, respectively]. This is important, because it has been suggested that for successful nerve regeneration after injury, axon regeneration must be both enhanced and directed to achieve re-integration with the host parenchyma[28] and these data suggest that both features are present in areas of astrocyte alignment.

Increased neurite growth within 3D tethered collagen gels is dependent on the presence of aligned astrocytes

To determine whether the increased neurite length was dependent on the presence of aligned astrocytes, or merely a fibroblast-aligned collagen matrix, dissociated DRGs were seeded into gels containing no astrocytes (fibroblasts only) in which all other parameters, for example, cell density, incubation time, and extent of gel contraction, remained constant. Neurite outgrowth appeared reduced in all regions compared with astrocyte gels despite taking on an aligned appearance in the gel edges [Fig. 6(i) A–C]. The percentage of neurites of different lengths was equivalent in both the delta zones and gel edges [Fig. 6(ii)], and there was no significant difference in the mean neurite length in any of the gel regions [Fig. 6(iii)]. Further, the number of neurites per neuronal cell body was significantly lower in all regions of the gels without astrocytes compared with that in gels with astrocytes (Supplemental Fig. S1, available online at www.liebertonline.com/ten), although the total number of neurons was comparable between the two types of gel. In addition, in gels with astrocytes, the mean number of neurites per neuronal cell body did not differ significantly between the delta zone, middle, and edge (Supplemental Fig. S1), indicating that the number of neurites does not change with alignment, only the neurite length. These data show that enhanced neurite outgrowth was dependent on the presence of astrocytes (specifically aligned astrocytes) and was not merely a result of an aligned collagen environment.

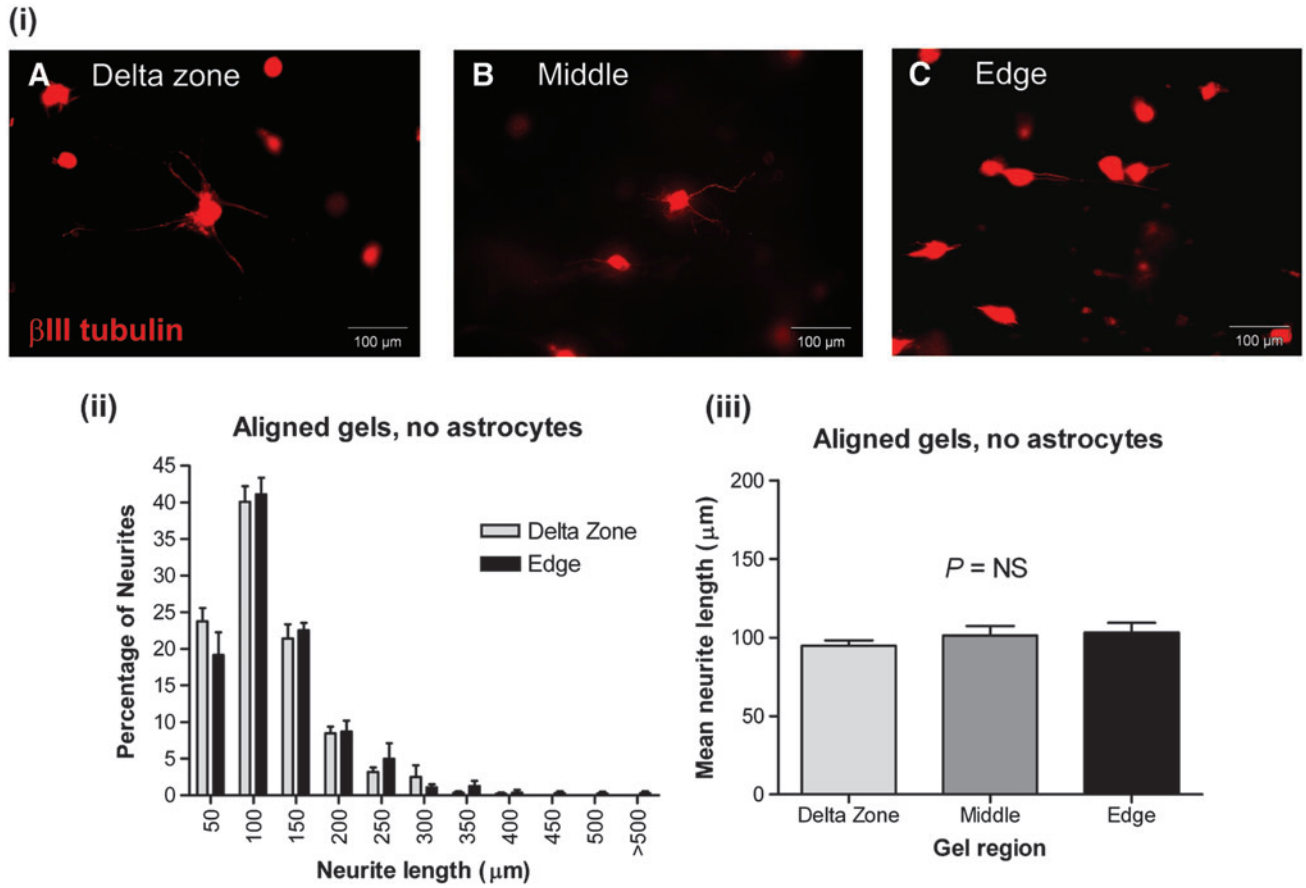

FIG. 6. In the absence of astrocytes, aligned gels do not promote neurite elongation. (**i**) Neurons stained for βIII tubulin within aligned tethered gels without astrocytes (fibroblast and DRGs only; **A–C**). (**ii**) Frequency distribution graph now shows no difference in neurite length between edge and delta zone regions of astrocyte-free aligned collagen gels. (**iii**) There was no significant difference in the mean neurite length in the different regions of tethered gels that were aligned but contained no astrocytes (only fibroblasts and DRGs). $n = 6$ independent gels. DRGs, dorsal root ganglias. Color images available online at www.liebertonline.com/ten.

Aligned astrocyte construct for implantation supports aligned neurite outgrowth

Since this work and other reports[13–16,28,37] demonstrate aligned astrocytes are conducive for enhanced and directed neuronal growth, we postulated that this could provide a novel basis for an implantable device to bridge spinal cord injuries. Previous studies have shown how cells in tethered aligned collagen gels can be delivered to peripheral nerve injury sites,[29] but the requirement for external tethering and overall fragility of such devices makes this unsuitable for clinical CNS repair. Here, we used plastic compression to transform the tethered aligned astrocyte gels into robust constructs that could be bundled together to form an implantable device. After plastic compression of tethered aligned gels, there was no significant increase in cell death compared with uncompressed controls ($10.21\% \pm 2.43\%$ vs. $10.27\% \pm 0.65\%$; Supplemental Fig. S2, available online at www.liebertonline.com/ten). Thus, astrocytes remained viable and retained their aligned conformation (Fig. 7A) after the removal of external tethering. DRG neurons were cultured on these constructs to assess their ability to support and direct neuronal growth. Fluorescence microscopy suggested that neurites extended along the processes of astrocytes within these constructs, and this was subsequently confirmed by confocal microscopy (Fig. 7B–D).

Discussion

The tethered self-aligning collagen gel system provides a robust and reproducible 3D model in which the effect of astrocyte alignment on neurite outgrowth can be investigated in a more spatially relevant way than in previous *in vitro* studies. Increased neurite outgrowth correlated to areas of greatest astrocyte alignment, either when neurons were seeded on the surface or within tethered astrocyte gels. Further, the enhancement of neurite outgrowth was lost when astrocytes were removed from the system, suggesting that this effect is dependent on the specific presence of aligned astrocytes, and does not merely require matrix alignment. This is important, as nervous system repair devices are typically anisotropic to guide neuronal growth cones directly through a lesion and tend to be surrounded by astrocytes rather than penetrated by them. This demonstration in a 3D environment of a phenomenon that had only been previously seen in 2D cultures (and was impossible to isolate using animal models) highlights the importance of astrocyte alignment as a possible future therapeutic intervention for SCI repair and suggests that future CNS repair devices might usefully encourage host astrocyte infiltration provided that it is aligned.

In previous studies, outgrowth of DRG neurons was enhanced on aligned astrocyte-seeded polydioxanone fibers, compared with unaligned fibers and those without astrocytes,[37] and aligned astrocytes in monolayer culture were sufficient to direct and enhance neurite outgrowth.[16] Further, these engineered monolayers expressed linear arrays of astrocyte-derived adhesive and repulsive ligands, including laminin, fibronectin, and CSPGs, suggesting that the particular arrangement of these molecules may be important to direct nerve regeneration.[16] In accordance with these studies, we also found that astrocyte alignment was sufficient to direct and enhance neurite outgrowth and likewise observed some areas of CSPG alignment, the main difference being that we identified these features in 3D cultures. This observation is similar to *in vivo* studies where undamaged white matter tracts can support neurite growth parallel to their longitudinal axis despite the presence of growth inhibitors such as CSPGs (reviewed by Ref.[38]), implying that the inhibitory nature of the glial scar may be overcome by reconfiguring cellular alignment.

Enhancement of neurite outgrowth (length and number of neurites) was dependent on the presence of the astrocytes.

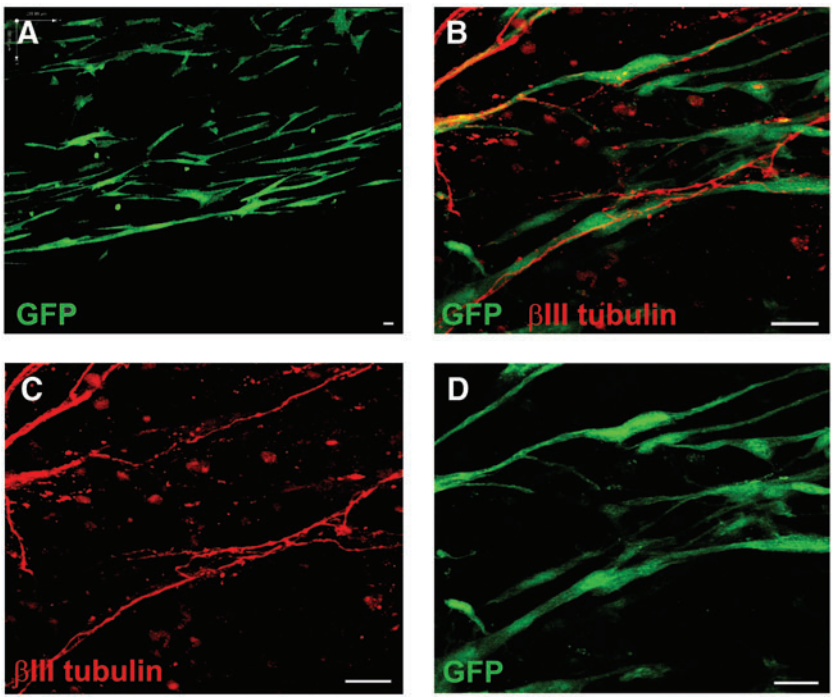

FIG. 7. Neurite outgrowth is guided by aligned astrocytes in implantable plastic compressed collagen conduits. Astrocytes in plastic compressed devices survived and remained aligned within the matrix (**A**)—GFP. High magnification confocal microscopy was performed on plastic compressed aligned astrocyte devices that had DRGs seeded onto them (**B–D**). Neurites stained for βIII tubulin could be seen extending along GFP astrocyte processes. Scale bars = 25 μm. GFP, green fluorescent protein. Color images available online at www.liebertonline.com/ten.

Astrocytes can express neurite growth, promoting cell surface molecules such as N-cadherin and neural cell adhesion molecule (NCAM),[39] and the arrangement of these molecules on the astrocyte surface appears to be important for robust neurite growth.[16] In addition, astrocytes can secrete proteins to increase neuronal length, branching and synaptogenesis including cholesterol:Apolipoprotein E complex[40] thrombospondins,[41] and other as yet unidentified proteins that were neither of the above, nor neurotrophins.[42] It would be interesting to investigate expression and arrangement of these proteins using the culture model we developed. In a study by Alexander *et al.*,[28] astrocytes were aligned through the application of an electrical field in 2D cultures. As these authors point out, when a single directional cue is absent, the growth cone must constantly sample the microenvironment to determine the optimal direction of growth, which takes time due to the assembly and disassembly of cytoskeletal proteins. Conversely, when a unidirectional cue is present, the process is more efficient, enhancing rate of neurite extension. This may explain why neurite growth in the aligned regions of our astrocyte-seeded gels was greater than in the unaligned delta zones at the end of the 3-day incubation period.

Although this study allowed robust and detailed *in vitro* investigation into the effect of astrocyte alignment on neurite outgrowth, further work is required to assess the effectiveness of the approach, particularly investigating the maturity and source of the astrocytes and type of neurons. This is an important step before *in vivo* testing, as CNS and peripheral nervous system neurons show intrinsic and age-dependent differences in their regenerative abilities.[43]

Having established that an aligned 3D astrocyte environment is conducive to supporting and guiding neuronal growth, a device was developed and tested with a view to engineering an aligned astrocyte guide for implantation into a spinal cord lesion *in vivo*. This is in contrast to many current bridging devices aimed at SCI repair that contain Schwann cells, which can themselves trigger astrocytes to become growth inhibitory,[44,45] preventing axons from crossing the Schwann cell-astrocyte transition zone.[46] Using astrocytes in a graft may, therefore, lessen the response of surrounding astrocytes and minimize glial scarring, because axons grow well in the undamaged spinal cord.[47,48] Before we can explore this approach *in vivo*, it was important to develop an implantable device in which astrocytes were maintained in their aligned supportive arrangement. We demonstrate that plastic compression of aligned astrocyte 3D collagen gels is one means to engineer fibers of aligned astrocytes many millimeter long and of appropriate diameter, which could be packed together to form an implantable conduit. Neuronal outgrowth on the surface of these fibers followed the guidance provided by the astrocyte processes, demonstrating the usefulness of this approach for spinal cord repair. Further development of this technology will require an appropriate source of astrocytes (or an alternative cell type with appropriate properties) and, although type I collagen devices have been shown to improve recovery of motor function after SCI,[49–51] this protein is not normally found in the mammalian CNS. Our future studies will, therefore, also explore the possibility of substituting type I collagen with other protein hydrogels to identify optimal materials for this approach (review of biomaterial approaches[52]).

In addition to developing implantable aligned astrocyte environments, attempts to align the endogenous glial scar may provide a useful therapeutic intervention, as the 3D culture work suggests that it is not the reactivity of astrocytes *per se* that is inhibitory, rather more their disordered organization. An *in vivo* study[9] demonstrated that implanted astrocytes derived from embryonic glial-restricted precursors promoted robust axon growth and restoration of locomotor function after acute transection injuries in the adult rat spinal cord. Histological analysis revealed parallel alignment and interweaving of implanted glial-restricted precursor processes with host GFAP positive processes, creating an aligned environment of glial surfaces. Additionally, Hofstetter *et al.*[10] implanted marrow stromal cells in an injured rat spinal cord that colocalized with longitudinally aligned astrocyte processes and supported neuronal growth. These studies provide further evidence that alignment of glial scar astrocytes *in vivo* is associated with successful neuronal regeneration.

In summary, using advanced 3D cell culture techniques, we have shown that astrocyte alignment enhances and directs neurite outgrowth in a system where it was possible to isolate this single variable. This new model system provides a powerful tool by which the effects of graded anisotropy within distinct populations of CNS cells in coculture can be studied in a highly controlled and well-defined environment over a period of time. Further, we have combined self-alignment of a cellular collagen hydrogel with plastic compression to yield a novel method for assembling aligned cellular constructs suitable for tissue engineering.

Acknowledgment

This work was supported by the Wellcome Trust (080309).

Disclosure Statement

The authors have no competing financial interests.

References

1. Suzuki, M., and Raisman, G. The glial framework of central white matter tracts: segmented rows of contiguous interfascicular oligodendrocytes and solitary astrocytes give rise to a continuous meshwork of transverse and longitudinal processes in the adult rat fimbria. Glia **6,** 222, 1992.
2. Yiu, G., and He, Z. Glial inhibition of CNS axon regeneration. Nat Rev Neurosci **7,** 617, 2006.
3. Fawcett, J.W., and Asher, R.A. The glial scar and central nervous system repair. Brain Res Bull **49,** 377, 1999.
4. Liu, B.P., Cafferty, W.B., Budel, S.O., and Strittmatter, S.M. Extracellular regulators of axonal growth in the adult central nervous system. Philos Trans R Soc Lond B Biol Sci **361,** 1593, 2006.
5. Geller, H.M., and Fawcett, J.W. Building a bridge: engineering spinal cord repair. Exp Neurol **174,** 125, 2002.
6. Reier, P.J. Penetration of grafted astrocytic scars by regenerating optic nerve axons in *Xenopus* tadpoles. Brain Res **164,** 61, 1979.
7. Singer, M., Nordlander, R.H., and Egar, M. Axonal guidance during embryogenesis and regeneration in the spinal cord of the newt: the blueprint hypothesis of neuronal pathway patterning. J Comp Neurol **185,** 1, 1979.

8. Li, Y., Field, P.M., and Raisman, G. Regeneration of adult rat corticospinal axons induced by transplanted olfactory ensheathing cells. J Neurosci **18,** 10514, 1998.
9. Davies, J.E., Huang, C., Proschel, C., Noble, M., Mayer-Proschel, M., and Davies, S.J. Astrocytes derived from glial-restricted precursors promote spinal cord repair. J Biol **5,** 7, 2006.
10. Hofstetter, C.P., Schwarz, E.J., Hess, D., Widenfalk, J., El Manira, A., Prockop, D.J., *et al.* Marrow stromal cells form guiding strands in the injured spinal cord and promote recovery. Proc Natl Acad Sci U S A **99,** 2199, 2002.
11. Davies, S.J., Field, P.M., and Raisman, G. Regeneration of cut adult axons fails even in the presence of continuous aligned glial pathways. Exp Neurol **142,** 203, 1996.
12. East, E., and Phillips, J.B. Tissue engineered cell culture models for nervous system research. In: Greco, G.N., ed. Tissue Engineering Research. New York, NY: Nova Science Publishers, 2008, pp. 141–160.
13. Sorensen, A., Alekseeva, T., Katechia, K., Robertson, M., Riehle, M.O., and Barnett, S.C. Long-term neurite orientation on astrocyte monolayers aligned by microtopography. Biomaterials **28,** 5498, 2007.
14. Recknor, J.B., Recknor, J.C., Sakaguchi, D.S., and Mallapragada, S.K. Oriented astroglial cell growth on micropatterned polystyrene substrates. Biomaterials **25,** 2753, 2004.
15. Recknor, J.B., Sakaguchi, D.S., and Mallapragada, S.K. Growth and differentiation of astrocytes and neural progenitor cells on micropatterned polymer films. Ann N Y Acad Sci **1049,** 24, 2005.
16. Biran, R., Noble, M.D., and Tresco, P.A. Directed nerve outgrowth is enhanced by engineered glial substrates. Exp Neurol **184,** 141, 2003.
17. Silver, J., and Miller, J.H. Regeneration beyond the glial scar. Nat Rev Neurosci **5,** 146, 2004.
18. Pampaloni, F., Reynaud, E.G., and Stelzer, E.H. The third dimension bridges the gap between cell culture and live tissue. Nat Rev Mol Cell Biol **8,** 839, 2007.
19. Brown, R.A., and Phillips, J.B. Cell responses to biomimetic protein scaffolds used in tissue repair and engineering. Int Rev Cytol **262,** 75, 2007.
20. Lee, J., Cuddihy, M.J., and Kotov, N.A. Three-dimensional cell culture matrices: state of the art. Tissue Eng Part B Rev **14,** 61, 2008.
21. James Kirkpatrick, C., Fuchs, S., Iris Hermanns, M., Peters, K., and Unger, R.E. Cell culture models of higher complexity in tissue engineering and regenerative medicine. Biomaterials **28,** 5193, 2007.
22. Pedersen, J.A., and Swartz, M.A. Mechanobiology in the third dimension. Ann Biomed Eng **33,** 1469, 2005.
23. East, E., Golding, J.P., and Phillips, J.B. A versatile 3D culture model facilitates monitoring of astrocytes undergoing reactive gliosis. J Tissue Eng Regen Med **3,** 634, 2009.
24. Cullen, D.K., Simon, C.M., and LaPlaca, M.C. Strain rate-dependent induction of reactive astrogliosis and cell death in three-dimensional neuronal-astrocytic co-cultures. Brain Res **1158,** 103, 2007.
25. Ceballos, D., Navarro, X., Dubey, N., Wendelschafer-Crabb, G., Kennedy, W.R., and Tranquillo, R.T. Magnetically aligned collagen gel filling a collagen nerve guide improves peripheral nerve regeneration. Exp Neurol **158,** 290, 1999.
26. Dubey, N., Letourneau, P.C., and Tranquillo, R.T. Guided neurite elongation and Schwann cell invasion into magnetically aligned collagen in simulated peripheral nerve regeneration. Exp Neurol **158,** 338, 1999.
27. Lanfer, B., Freudenberg, U., Zimmermann, R., Stamov, D., Korber, V., and Werner, C. Aligned fibrillar collagen matrices obtained by shear flow deposition. Biomaterials **29,** 3888, 2008.
28. Alexander, J.K., Fuss, B., and Colello, R.J. Electric field-induced astrocyte alignment directs neurite outgrowth. Neuron Glia Biol **2,** 93, 2006.
29. Phillips, J.B., Bunting, S.C., Hall, S.M., and Brown, R.A. Neural tissue engineering: a self-organizing collagen guidance conduit. Tissue Eng **11,** 1611, 2005.
30. Eastwood, M., Mudera, V.C., McGrouther, D.A., and Brown, R.A. Effect of precise mechanical loading on fibroblast populated collagen lattices: morphological changes. Cell Motil Cytoskeleton **40,** 13, 1998.
31. Dutton, G.R., Currie, D.N., and Tear, K. An improved method for the bulk isolation of viable perikarya from postnatal cerebellum. J Neurosci Methods **3,** 421, 1981.
32. Phillips, J.B., King, V.R., Ward, Z., Porter, R.A., Priestley, J.V., and Brown, R.A. Fluid shear in viscous fibronectin gels allows aggregation of fibrous materials for CNS tissue engineering. Biomaterials **25,** 2769, 2004.
33. Phillips, J.B., and Brown, R.A. Self-aligning tissue growth guide. Patent number WO/2004/087231, 2004.
34. Brown, R.A., Wiseman, M., Chuo, C.-B., Cheema, U., and Nazhat, S.N. Ultrarapid engineering of biomimetic materials and tissues: fabrication of nano- and microstructures by plastic compression. Adv Funct Mat **15,** 1762, 2005.
35. Brown, R.A., Nazhat, S.N., Mudera, V., and Wiseman, M. Cell-independent fabrication of tissue equivalents. Patent number WO/2006/003442, 2006.
36. Kwok, J.C., Afshari, F., Garcia-Alias, G., and Fawcett, J.W. Proteoglycans in the central nervous system: plasticity, regeneration and their stimulation with chondroitinase ABC. Restor Neurol Neurosci **26,** 131, 2008.
37. Chow, W.N., Simpson, D.G., Bigbee, J.W., and Colello, R.J. Evaluating neuronal and glial growth on electrospun polarized matrices: bridging the gap in percussive spinal cord injuries. Neuron Glia Biol **3,** 119, 2007.
38. Nishio, T. Axonal regeneration and neural network reconstruction in mammalian CNS. J Neurol **256 Suppl 3,** 306, 2009.
39. Neugebauer, K.M., Tomaselli, K.J., Lilien, J., and Reichardt, L.F. N-cadherin, NCAM, and integrins promote retinal neurite outgrowth on astrocytes *in vitro*. J Cell Biol **107,** 1177, 1988.
40. Mauch, D.H., Nagler, K., Schumacher, S., Goritz, C., Muller, E.C., Otto, A., *et al.* CNS synaptogenesis promoted by glia-derived cholesterol. Science **294,** 1354, 2001.
41. Christopherson, K.S., Ullian, E.M., Stokes, C.C., Mullowney, C.E., Hell, J.W., Agah, A., *et al.* Thrombospondins are astrocyte-secreted proteins that promote CNS synaptogenesis. Cell **120,** 421, 2005.
42. Hughes, E.G., Elmariah, S.B., and Balice-Gordon, R.J. Astrocyte secreted proteins selectively increase hippocampal GABAergic axon length, branching, and synaptogenesis. Mol Cell Neurosci **43,** 136, 2010.
43. Fawcett, J.W., Housden, E., Smith-Thomas, L., and Meyer, R.L. The growth of axons in three-dimensional astrocyte cultures. Dev Biol **135,** 449, 1989.
44. Adcock, K.H., Brown, D.J., Shearer, M.C., Shewan, D., Schachner, M., Smith, G.M., *et al.* Axon behaviour at Schwann cell—astrocyte boundaries: manipulation of axon signalling pathways and the neural adhesion molecule L1 can enable axons to cross. Eur J Neurosci **20,** 1425, 2004.

45. Wilby, M.J., Muir, E.M., Fok-Seang, J., Gour, B.J., Blaschuk, O.W., and Fawcett, J.W. N-Cadherin inhibits Schwann cell migration on astrocytes. Mol Cell Neurosci **14,** 66, 1999.
46. Golding, J.P., and Cohen, J. Border controls at the mammalian spinal cord: late-surviving neural crest boundary cap cells at dorsal root entry sites may regulate sensory afferent ingrowth and entry zone morphogenesis. Mol Cell Neurosci **9,** 381, 1997.
47. Davies, S.J., Fitch, M.T., Memberg, S.P., Hall, A.K., Raisman, G., and Silver, J. Regeneration of adult axons in white matter tracts of the central nervous system. Nature **390,** 680, 1997.
48. Davies, S.J., Goucher, D.R., Doller, C., and Silver, J. Robust regeneration of adult sensory axons in degenerating white matter of the adult rat spinal cord. J Neurosci **19,** 5810, 1999.
49. Joosten, E.A., Veldhuis, W.B., and Hamers, F.P. Collagen containing neonatal astrocytes stimulates regrowth of injured fibers and promotes modest locomotor recovery after spinal cord injury. J Neurosci Res **77,** 127, 2004.
50. Yara, T., Kato, Y., Kataoka, H., Kanchiku, T., Suzuki, H., Gondo, T., *et al.* Environmental factors involved in axonal regeneration following spinal cord transection in rats. Med Mol Morphol **42,** 150, 2009.
51. Yoshii, S., Oka, M., Shima, M., Akagi, M., and Taniguchi, A. Bridging a spinal cord defect using collagen filament. Spine (Phila Pa 1976) **28,** 2346, 2003.
52. Norman, L.L., Stroka, K., and Aranda-Espinoza, H. Guiding axons in the central nervous system: a tissue engineering approach. Tissue Eng Part B Rev **15,** 291, 2009.

Address correspondence to:
Emma East, Ph.D.
Department of Life Sciences
The Open University
Walton Hall
Milton Keynes MK7 6AA
United Kingdom

E-mail: e.east@open.ac.uk

Received: January 11, 2010
Accepted: May 21, 2010
Online Publication Date: July 13, 2010